Eye (2016) 30, 1509–1516

www.nature.com/eye

LABORATORY STUDY

Optical coherence tomography characteristics of different types of big bubbles seen in deep anterior lamellar keratoplasty by the big bubble technique

SL AlTaan[1], K Termote[2,3], MS Elalfy[1], E Hogan[1], R Werkmeister[4], L Schmetterer[4,5], S Holland[2] and HS Dua[1]

Abstract

Purpose **To define optical coherence tomography (OCT) characteristics of type-1, type-2, and mixed big bubbles (BB) seen in deep anterior lamellar keratoplasty.**

Methods **Human sclero-corneal discs were obtained from UK (30) and Canada (16) eye banks. Air was injected into corneal stroma until a BB formed. UK samples were fixed in formalin before scanning with Fourier-domain (FD-OCT). One pair of each type of BB was scanned fresh. All BB obtained from Canada were scanned fresh with time-domain (TD-OCT). For each OCT machine used, type-1 BB from which Descemets membrane (DM) was partially peeled, were also scanned. The morphological characteristics of the scans were studied.**

Results **FD-OCT of the posterior wall of type-1 (Dua's layer (DL) with DM) and type-2 BB (DM alone) both revealed a double-contour hyper-reflective curvilinear image with a hypo-reflective zone in between. The anterior line of type-2 BB was thinner than that seen with type-1 BB. In mixed BB, FD-OCT showed two separate curvilinear images. The anterior image was a single hyper-reflective line (DL), whereas the posterior image, representing the posterior wall of type-2 BB (DM) was made of two hyper-reflective lines with a dark space in between. TD-OCT images were similar with less defined component lines, but the entire extent of the BB could be visualised.**

Conclusion **On OCT examination the DM and DL present distinct features, which can help identify type-1, type-2, and mixed BB. These characteristics will help corneal surgeons interpret intraoperative OCT during lamellar corneal surgery.**

Eye (2016) **30,** 1509–1516; doi:10.1038/eye.2016.129; published online 29 July 2016

Introduction

Deep anterior lamellar keratoplasty (DALK) is considered the gold standard procedure for corneal transplantation where best corrected vision is affected by scars, dystrophy, or ectasia involving corneal stroma. The most popular technique is big bubble (BB) technique,[1] wherein air is injected in the corneal stroma to separate either Descemet's membrane (DM) or DM together with a layer of deep corneal stroma termed as pre-Descemet's layer (Dua's layer, DL). This allows replacement of affected stroma with healthy stroma from a cadaver donor. Injection of air into human corneal stroma produces three different types of BB:[2] (1) Type-1, where air cleaves along anterior surface of DL separating it from the deep posterior stroma; BB starts at the centre and spreads centrifugally to a maximum diameter of 8.5 mm. (2) Type-2, where air cleaves DM from stroma. This type starts from corneal periphery and spreads across the posterior surface of the cornea reaching a maximum diameter of 10–10.5 mm. (3) Mixed BB, where both type-1 and type-2 appear together. Usually type-1 is complete and type-2 is partial. Rarely both are complete with type-2 enclosing type-1 within.[2,3]

Knowing which type has formed intra-operatively is very important as type-2 and type-2 component of a mixed BB are vulnerable to tearing or bursting. This can be avoided by

[1]Larry A Donoso Laboratory for Eye Research, Section of Ophthalmology, Division of Clinical Neuroscience, University of Nottingham, Nottingham, UK

[2]University of British Columbia Vancouver, Vancouver, BC, Canada

[3]Department of Ophthalmology, University Hospital Brussels, Brussels, Belgium

[4]Center for Medical Physics and Biomedical Engineering, Medical University of Vienna, Vienna, Austria

[5]Department of Clinical Pharmacology, Medical University of Vienna, Austria

Correspondence: HS Dua, Academic Ophthalmology, B Floor, Eye ENT Centre, Queens Medical Centre, Derby Road, Nottingham NG7 2UH, UK
Tel: +44 (0)115 849 3354; Fax: +44 (0)115 970 9963.
E-mail: Harminder.Dua@nottingham.ac.uk

Received: 17 February 2016
Accepted in revised form: 1 May 2016
Published online: 29 July 2016

taking necessary precautions. Clinical clues such as the point of origin and BB size as described above and the 'rough' appearance of the wall of type-1 seen after excising the stroma compared to very smooth appearance of type-2 (ref. 4) help to distinguish type-1 from type-2. Recognising mixed BB intra-operatively is difficult. Anecdotal presentations at meetings of images from intraoperative optical coherence tomography (OCT) have indicated that this might be the definitive way of recognising the different types of BB. OCT offers non-contact, real time, cross-sectional images, which were hitherto impossible to acquire.[5–7] Since its introduction in 1994 by Izatt *et al*, anterior segment OCT has become an essential tool in clinical diagnosis and follow up of many ocular pathologies.[8–10] OCT of anterior segment provides image resolution of 1–15 μm in both axial and lateral directions. This resolution is finer than conventional imaging modalities, such as ultrasound, magnetic resonance imaging (MRI), or computed tomography.[7,11] Furthermore, image acquisition does not require topical anaesthesia or a water bath.[12–14] Two types of OCT are in common use, time-domain (TD-OCT) and Fourier-domain (FD-OCT). TD-OCT (Visante, Carl Zeiss Meditec AG, Jena, Germany) has a resolution of 18 μm and scan speed of 2048A-scans per second. FD-OCT (Spectralis, Heidelberg, Germany and Topcon, Tokyo, Japan), which can provide more detailed cross-sectional images of the biological structures, has an axial resolution of 5 μm and at least ten times faster scan speed.

In this study we undertook OCT examination and analysis of different types of BB created in eye bank donor eyes[15] and ascertained characteristics, which will enhance our understanding of the BB anatomy and inform and help surgeons to interpret real-time OCT images during DALK and other posterior segment surgery.

Materials and methods

Thirty human sclero-corneal discs maintained in organ culture in Eagle's minimum essential medium with 2% foetal bovine serum for 4–8 weeks post-mortem were used for scanning with Spectralis and Topcon OCT systems. Donor details (age, sex, and cause of death) are given in Table 1. Donor tissue was obtained from National Health Service Blood and Tissue (NHSBT) eyebank, Manchester, UK.

Air injection

The sclero-corneal discs were removed from storage medium and placed in a petri-dish, endothelium-side up, and covered with balanced salt solution. Under an operating microscope, a 30-gauge needle, bevel-up, attached to a 5-ml syringe was passed from the scleral rim into the corneal stroma and advanced to the centre of the disc. The needle was passed close to endothelial surface without perforating it. Air was injected with force to overcome the tissue resistance, until a big bubble was formed. All BBs were obtained in one attempt. When the syringe was emptied of air without a BB forming, the syringe was disengaged from the needle, whereas the needle remained in the stroma. The syringe was re-filled with air, re-connected to the needle and more air injected to form a BB. The BB type was ascertained and the samples fixed in 10% formalin. Two samples of each type of BB were scanned without fixation and compared to images obtained from formalin fixed samples.

OCT

Twelve samples (3 type-1, 3 type-2, 3 mixed, and 3 type-1 from which DM had been partially peeled) were examined with Topcon OCT (3D-OCT-2000) system (Topcon Corporation). Eighteen samples (5 type-1, 3 type-2, 6 mixed, and 4 type-1 from which DM had been partially peeled) were examined with Spectralis OCT (Spectralis).

A special clamp with a long flexible arm that could be affixed to the OCT table or head-rest frame at one end and a ball-and-socket type joint allowing movement in any direction attached to an artificial anterior chamber (AAC) holder at the other end was used. The sclero-corneal disc with the posterior surface out (surface with BB) was mounted on AAC (Katena, Denville, NJ, USA), the chamber was filled with BSS and AAC tubing was closed. AAC carrying the sample was mounted in the holder and positioned such that BB was perpendicular to the objective of OCT equipment. Using 'Cornea' mode of OCT machine, BB was scanned to get average 10 scans per sample. Representative scans were selected and the thickness of BB wall and its components were measured using equipment software.

Sixteen additional samples (5 type-1, 4 type-2, 3 mixed, and 4 type-1 from which DM was partially peeled) from University of British Columbia, Vancouver, were examined with the Visante OCT system (Carl Zeiss Meditec AG). This provided wide angle images of BB. These samples were stored in Optisol (Chiron Ophthalmics, Irvine, California) at 4 °C. OCT imaging was performed soon after air inflation in these samples. As with previous examinations, samples were scanned with BB facing the OCT system. Images were captured using 'Enhanced Anterior Segment Single' mode and exported to image-J for evaluation. Mean and standard deviation of measurements from all scans were calculated, for each instrument used. Donor details are given in Table 1.

Table 1 Donor information for the sclero-corneal samples obtained from the National Health Service Blood and Transplant (NHSBT), UK eye banks, and from the University of British Columbia, Vancouver, Canada

NHSBT, UK				*University of British Columbia, Vancouver, Canada*			
Sample Number	*Sex*	*Age (years)*	*Cause of death*	*Sample Number*	*Sex*	*Age (years)*	*Cause of Death*
E875	F	56	Renal cancer	0071OD	M	51	Lung cancer
M17915B	F	93	Pneumonia	0189OD	M	53	Cardiac arrest
E18037A	Unknown	Unknown	Unknown	0189OS	M	53	Cardiac arrest
E917	F	69	Intracranial heamorrhage	0294	F	42	Cerebrovascular accident
E948	M	79	Pneumonia	0030OD	M	63	Squamous cell carcinoma
E1208	M	66	Unknown (other)	0059OS	F	71	Peritoneal carcinoma
E1046	Unknown	Unknown	Unknown	0260	M	63	Renal carcinoma
E1132	M	76	Cancer	0233OS	F	63	Lung carcinoma
E1170	F	80	Unknown (other)	0233OD	F	63	Lung carcinoma
E877	F	92	COPD	0059OD	F	71	Peritoneal carcinoma
E1072	M	84	Pancreatitis	0214	M	55	Pancreatic carcinoma
E1074	F	93	Dementia	0352	F	65	Cancer
E1881	M	60	Unknown (other)	0071OD	M	51	Lung cancer
E1911	F	83	Pneumonia	0189OD	M	53	Cardiac arrest
E1914	F	67	Unknown (other)	0189OS	M	53	Cardiac arrest
E1950	M	82	Lung cancer	0294	F	42	Cerebrovascular accident
E1985	F	74	Unknown (other)				
E1959	Unknown	Unknown	Unknown				
E1879	M	78	Unknown (other)				
E1878	M	78	Unknown (other)				
E1856	M	79	Chronic pulmonary disease				
E1839	M	65	Pneumonia				
E1910	F	83	Pneumonia				
E1909	M	89	Pneumonia				
E1917	F	75	Respiratory failure				
E1954	F	78	Encephalopathy				
E2030	M	76	Unknown (other)				
E2054	M	69	Pneumonia				
E2051	F	82	Cerebrovascular accident				
E1854	F	78	Respiratory failure				

Results

For NHSBT eyes, mean donor age was 70 years. There were 13 males and 14 females. Information was not available for three donor eyes. Cause of death varied and in some it was unknown and coded as 'other'. Mean donor age was 57 years for Vancouver donor eyes. There were nine males and seven females. In type-1, both Topcon and Spectralis OCTs of the posterior wall revealed parallel, double-contour, hyper-reflective curved line with a hypo-reflective space in between (Figures 1a and 2a). In type-2, OCT also revealed a parallel, double-contour curved hyper-reflective line with a dark space in between (Figures 1b and 2b), but the anterior line was narrower than that seen with a type-1 (Figures 1a and 2a). In the mixed BB, OCT showed two separate curvilinear images (Figures 1c and 2c) one with double-contour and the other as single hyper-reflective image. When DM was peeled-off type-1, OCT showed only single hyper-reflective curved line corresponding to part of the anterior line of the double-contour line described above (Figures 1d and 2d). On the other hand, Visante OCT of the posterior wall of type-1 and type-2 BB showed a single hyper-reflective curved line rather than the double-contour line. However, it captured the entire bubble diameter, whereas with FD-OCT only part of BB could be imaged at any one time (Figure 3).

Topcon OCT measurements are shown in Table 2. The mean thickness of DM was 41.54+/ − 2.79 μm and that of DL was 24.33+/ − 2.86 μm. However, the mean of DL+DM was 49.66+/ − 5.37 μm, which was not the sum of DL and DM separately. Also, results showed that the mean of DL+DM banded zone (DMB), which represents the anterior line of the posterior wall of type-1, was 18.11+/ − 1.64 μm, whereas the anterior line of type-2 measured 16.77+/ − 1.59 μm, which is slightly less than that of DL+DMB. Furthermore, the mean thickness of DL in mixed BB and peeled part of type-1 was 26+/ − 2.82 μm and 22.66+/ − 1.6 μm, respectively.

Spectralis OCT measurements are shown in Table 2. The mean thickness of DM was 25.89+/ − 5.81 μm and that of DL was 19.13+/ − 3.32 μm. However, the mean of DL+DM was 36.7+/ − 4.6 μm, which is not the sum of DL and DM separately. Also, results showed that the mean of

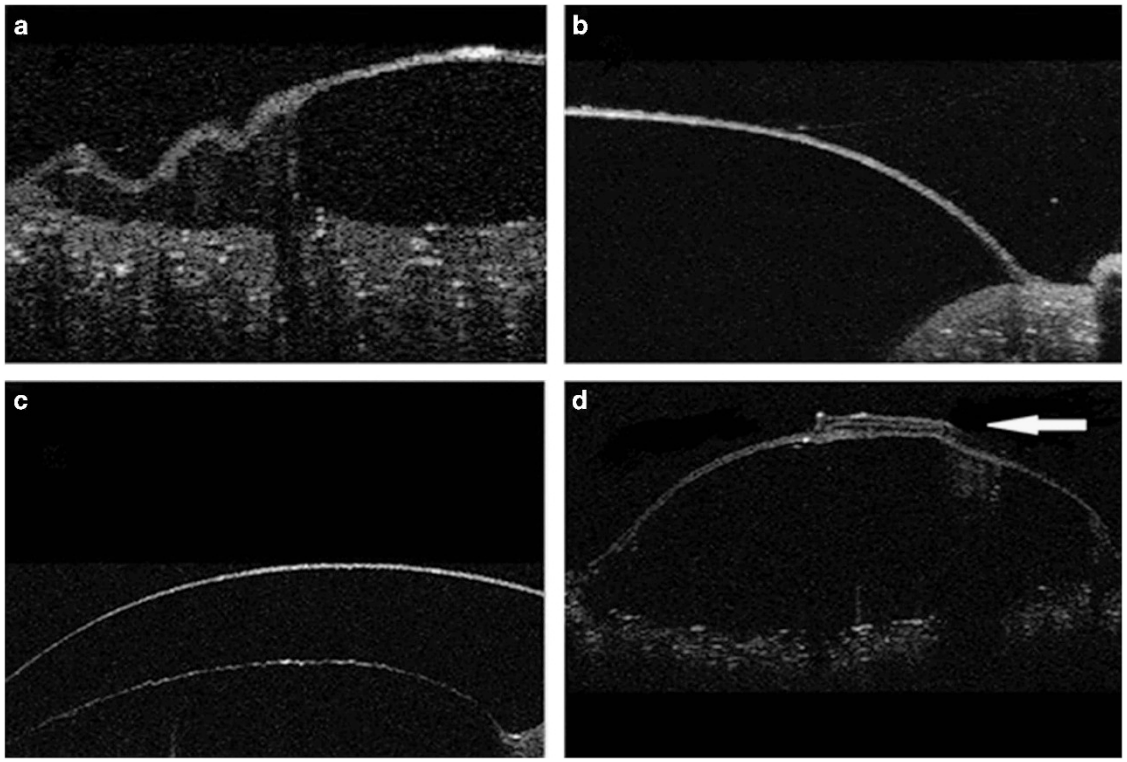

Figure 1 Topcon OCT: (a) Type-1 BB showing two curvilinear lines. The anterior line represents DL and banded zone of DM. (b) Type-2 BB showing two curvilinear lines that represent banded and non-banded zones of DM. (c) Mixed BB where the anterior line represents DL and the posterior line represents DM. (d) Type-1 BB from which the DM was partially peeled off. The peeled DM is folded on itself (arrow). The OCT image to the right of the peeled DM is a single line and that to the left has a double-contour as seen in the posterior wall of a type-1 BB.

DL+DMB, which represents the anterior line of a type-1 was 14.13+/− 2.47 μm, whereas the anterior line of a type-2 measured 10.44+/−0.95 μm, which is less than that of DL+DMB. Mean thickness of DL in mixed BB and the peeled part of type-1 was 18.78+/−2.6 μm and 19.6+/−4.1 μm, respectively.

Visante OCT measurements are shown in Table 2. All values were greater than those with the other two devices. Mean thickness of DM was 53.1+/−18.6 μm and that of DL was 51+/−15.6 μm. The mean of DL+DM was 72.6+/−15.5 μm, which is not the sum of DL and DM separately. The posterior wall of type-1 and type-2 BB presented as a single curvilinear hyper-reflective image unlike the corresponding images obtained with the other two devices. Mean thickness of DL in mixed BB and the peeled part of type-1 was 56.6+/−22.2 μm and 46.7+/−3.9 μm, respectively. No difference was noted in the samples measured 'fresh' and the same samples after fixation in formalin for up to 48 h.

Discussion

The BB technique is the most popular method used for DALK. Before the different types of BB were described, mechanism of BB formation were illunderstood.[2] Mixed BB as an entity was unknown and 'funny bubbles' were attributed to a split in banded and non-banded zones of the DM.[16] We now know that a type-1 BB is centrally located, has a tougher posterior wall, which can withstand high pressure and is not likely to tear or burst during surgery. When the posterior wall of a type-1 BB is inadvertently perforated, DALK can still be successfully completed as the tear does not extend. We now know that a mixed BB is due to the formation of types 1 and 2 simultaneously. In mixed BB the type-1 component is usually complete and the type-2 component is partial though both can be complete with the type-1 contained within the larger type-2. As the posterior wall of a type-2 BB and the type-2 component of a mixed BB are made of DM only they are vulnerable to large tears or bursts during surgery. As the type-2 BB margin extends close to the limbus, care has to be taken during performing paracentesis as the tip of the knife or needle can puncture the DM causing it to tear or burst. Although DALK can be successfully completed with both types 1 and 2 BBs; with a mixed BB the pocket of air between DL and the underlying DM often needs to be released with a fine needle puncture of the overlying DL.

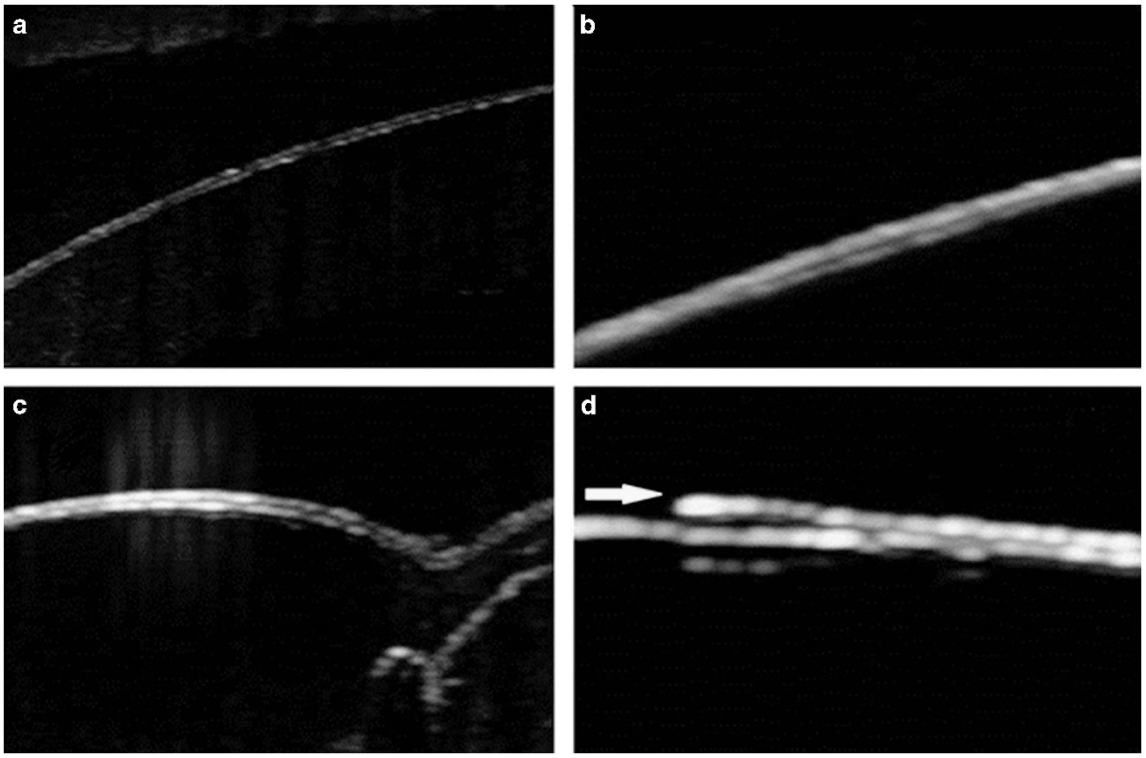

Figure 2 Spectralis OCT: (a) Type-1 BB two curvilinear lines exist. The anterior line represents DL and banded zone of DM. (b) Type-2 BB showing two curvilinear lines that represent banded and non-banded zones of DM. (c) The image is of the wall of the type-1 component of a partial mixed BB, where the anterior line represents DL and the posterior line represents DM. (d) Type-1 BB from which the DM was partially peeled off. The peeled DM is indicated by the arrow.

The clinical implications of the different types of BB make it imperative that the surgeon should be aware of the BB created during DALK. Details of the clinical implications of the different BB are described in a major review.[16] Intraoperative OCT can delineate the different BBs. Hence, it is important to ascertain the OCT characteristics of the BBs. We were able to reproduce the different BB types as reported by Dua *et al*.[2] OCT images could be obtained for all types of bubbles but the scan had to be performed with the posterior surface of BB facing the objective. This was due to the multitude of tiny bubbles or pockets of air in the corneal stroma, which created many artefacts and prevented acquisition of good images of the posterior wall of BB. Moreover, with FD-OCT the depth range of OCT system did not extend as far as the posterior wall of BB. Hence for consistency, with TD-OCT also, scanning was performed with the posterior wall facing the objective lens. In order to understand the description and measurements, it is therefore important to bear in mind that the convex surface of the OCT image of BB represents the posterior surface, and the concave surface of the image represents the anterior surface.

The characteristics of the images of the posterior wall of different BB examined were very similar for both Topcon and Spectralis equipment, but resolution was slightly better with Spectralis than with Topcon. The posterior wall of type-1, which is made of DL anteriorly and DM posteriorly and of type-2 made of DM alone were both seen as parallel, double-contour, curvilinear hyper-reflective images. The two hyper-reflective linear images were separated with narrow hypo-reflective dark line. In type-2 the anterior line was thinner than that seen in type-1. By direct observation it was difficult to discern which anatomical component contributed to which component of the OCT image.

On comparing the images of type-1 and type-2 BB, it was evident that DM independently produced a parallel, double-contour, hyper-reflective image with the two lines separated by dark space. By inference the two lines should therefore represent the banded zone (anterior line) and non-banded zone (with endothelium-posterior line) of DM. This observation has been reported with the use of ultrahigh-resolution OCT imaging of normal corneas and corneas with Fuch's endothelial dystrophy,[17–19] and is seen in OCT images reported by others but has not been specifically commented on.[20] In OCT image of type-1 BB, the anterior line would correspond to the banded zone and DL. Though this was thicker than that of the anterior line seen in type-2, the difference was only 2 (Spectralis) to 4 (Topcon) μm. The total thickness of the posterior wall

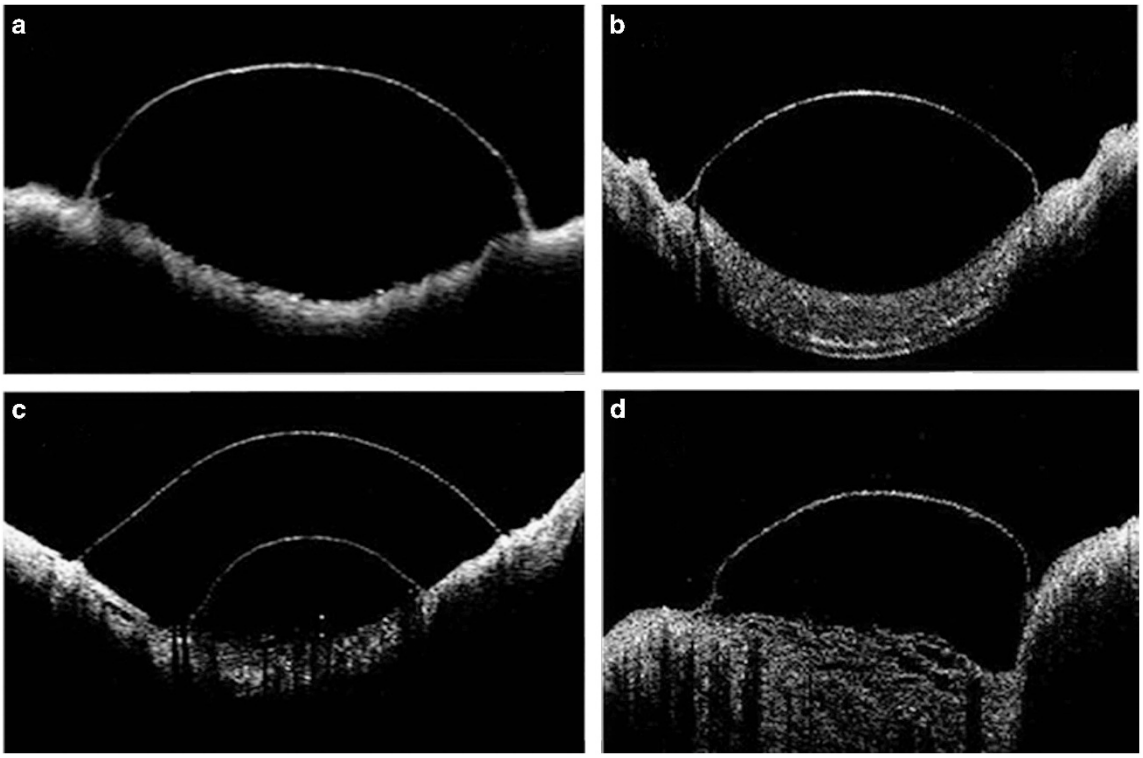

Figure 3 Visante OCT: (a) Type-1 BB where the single curvilinear line demarcated the entire extent of the BB. (b) Type-2 BB where the image is similar to that seen with a type-1 BB. (c) Mixed BB where the OCT scan was performed at the location of the two bubbles. The upper (posterior) line represents DM and the lower (anterior) line represents DL. The DM line does not demonstrate a 'double-contour' as is seen with the Topcon and Spectralis machines. (d) A type-1 BB from which DM was peeled off. The OCT image is similar to the DL image of a mixed BB.

of a type-1 BB was 36 (Spectralis) to 49 (Topcon) μm, whereas that of a type-2 was 25 (Spectralis) to 41 (Topcon) μm. This would be expected as the posterior wall of type-1 BB is made of DL+DM. Interestingly however, the thickness of DL alone as measured after peeling-off DM from type-1 or from mixed BB was 19 (Spectralis) to 24 (Topcon) μm producing an anomaly in that the sum of DL and DM measured individually did not add up to the thickness of the posterior wall of a type-1 BB, which is formed by these very same layers together. This could be due to inaccuracy in the measuring tool provided in the software of the equipment, especially in the range of thickness being measured or more likely to an artificial widening of the hyper-reflective images due to light backscatter.[7] This error could also be inherent in the automatic adjustment of the intensity scale applied by different equipment. Such artefactual widening would affect each layer individually thus amplifying the thickness measurement of each, making the sum of the two greater than the measure of the two layers closely applied to each other.

Dua *et al*[2] reported that DL measures around $10.15+/-3.6\,\mu$m on transmission electron microscopy.[2] The difference of this measurement from our OCT measurements is probably due to the fact that OCT images display biological tissue structure in a way different from the actual histological thickness. Moreover, measurements from histology sections do not accurately reflect the true thickness as tissue preparation for microscopic examination is associated with tissue dehydration. Fujimoto *et al*[7] state that 'In OCT, image contrast occurs from intrinsic differences in tissue optical properties. Thus, care must be taken when interpreting OCT images, since they are not analogous to conventional histology'. Furthermore, refraction at several boundaries, high index of the cornea and the added element of back reflection and scattering of light beam from corneal tissue would render OCT images thicker and different from histological images.[7,21]

The basis of mixed bubbles was first explained by Dua *et al*[2] who demonstrated that these were due to type-1 and type-2 BB occurring simultaneously with type-2 usually being partial and type-1 complete though both can be complete. Mixed BB had been observed by surgeons before the report by Dua *et al*, but were attributed to a split in banded and non-banded zones of DM. OCT images of mixed BB confirmed that the type-2 component was made of the full thickness of DM with parallel, double-contour line, and an additional single hyper-reflective image of

Table 2 OCT measurements of the posterior wall of the big bubbles obtained by Topcon, Spectralis, and Visante machines

Sample number	*Type of bubble*	*DL (μm)*	*DM (μm)*	*DL+DM (μm)*	*DL+DMB (μm)*	*DMB (μm)*
Topcon						
E875	T1BB			54	16	
M17915B	T1BB			48	18.33	
E18037A	T1BB			53	20	
E917	T2BB		40.3			16
E948	T2BB		39.33			19
E1208	T2BB		38.66			15.33
E1046	MB	24	41			
E1132	MB	30	43			
E1170	MB	24	47			
E877	PB	22		40		
E1072	PB	25		47		
E1074	PB	21		56		
Spectralis						
E1881	T1BB			34.3	13.3	
E1911	T1BB			34	14	
E1914	T1BB			36.3	16.6	
E1950	T1BB			28	10	
E1985	T1BB			38.3	16.6	
E1959	T2BB		29			10.33
E1879	T2BB		23.66			9.33
E1878	T2BB		39.6			11.66
E1856	MB	17	22			
E1839	MB	22	24			
E1910	MB	16	21			
E1909	MB	15.7	25.5			
E1917	MB	21	19			
E1954	MB	21	29.3			
E2030	PB	20.6				
E2054	PB	16		39		
E2051	PB	26		45		
E1854	PB	16		39		
Visante						
0030OD	T1BB			98		
0071OD	T1BB			80		
0189OD	T1BB			69		
0189OS	T1BB			64		
0294	T1BB			52		
0095OS	T2BB		28			
0233OD	T2BB		33			
0233OS	T2BB		75			
0260	T2BB		35			
0095OD	MB	32	65			
0214	MB	86	69			
0253	MB	52	67			
0071OD	PB	46				
00189OD	PB	46				
00189OS	PB	53				
0294	PB	42				

DL separated from DM by dark space (intervening air). When DM was partially peeled off type-1 BB, OCT image of the remaining underlying tissue (DL) revealed single hyper-reflective line similar to that of type-1 component of mixed BB. Adjacent unpeeled wall retained its double-contour configuration indicating that this was a feature of DM alone.

Visante OCT produced wide-field images of the bubbles, but the resolution of images was poor compared to the other two. In Visante images, DM appeared as a single hyper-reflective line. The measurement of thickness of the wall of type-1 with Visante OCT was 72.6+/−15.5 μm, which is much thicker than that obtained with other devices. Similarly, the thickness of DM and DL with Visante OCT was 53.1+/−18.6 μm and 51+/−15.6 μm, respectively, which were also much thicker than the measurements obtained from the other two devices. The low image resolution and higher backscatter intensity of light with Visante can explain the difference.

This study has enabled us to elucidate important OCT characteristics of the posterior layers of the cornea, which have implications for corneal surgery, especially with the advent of intraoperative OCT. Intraoperative OCT is proving to be a useful tool in aiding surgeons in a variety of procedures.[22,23] The study has also provided evidence to support clinical observations made in *ex-vivo* experiments on human eyes in particular with regard to the different types of bubbles and the nature of mixed BB. With the ongoing development of ultrahigh-resolution OCT and its introduction in clinical practice, direct observation both *in-vivo* and *ex-vivo*, of anatomical details of the cornea will be possible.

Summary

What was known before

- *In vitro* studies simulating DALK have demonstrated that two main types of big bubbles are formed when air is injected in the corneal stroma, namely the type-1 (cleavage occurs between DL and deep stroma) and the type-2 (cleavage occurs between DM and DL).
- In some instances both types of big bubbles occur simultaneously.
- This is termed the mixed bubble. Intra-operatively, it is difficult to judge clinically, which type of bubble has formed, especially the mixed bubble.
- Knowing which type of big bubble has formed is very useful to complete DALK successfully and foresee any intraoperative complications.

What this study adds

- OCT features elaborated in this study will aid surgeons to interpret intraoperative OCT images of the BB formed during surgery.
- It will inform the surgeon on the type of bubble(s) formed and enable him/her to plan the rest of the procedure accordingly.
- By exercising due care with mixed and type-2 BB complications such as rupture of the bubble can be avoided, making the surgery safer.

Conflict of interest

The authors declare no conflict of interest.

Acknowledgements

We would like to thank the Elizabeth C King Trust for the financial support.

References

1 Anwar M, Teichmann KD. Big-bubble technique to bare Descemet's membrane in anterior lamellar keratoplasty. *J Cataract Refract Surg* 2002; **28**: 398–403.
2 Dua HS, Faraj LA, Said DG, Gray T, Lowe J. Human corneal anatomy redefined: a novel pre-Descemet's layer (Dua's layer). *Ophthalmology* 2013; **120**: 1778–1785.
3 Dua HS, Faraj LA, Said DG. Dua's layer: its discovery, characteristics and clinical applications. In: del Buey A, Sayas MA *et al. Biomechanica y Arquitetura Corneal*. Elsevier: Barcelona, 2014, pp 35–47.
4 Dua HS, Katamish T, Said DG, Faraj LA. Differentiating type 1 from type 2 big bubbles in deep anterior lamellar keratoplasty. *Clin Ophthalmol* 2015; **9**: 1155–1157.
5 Lim SH. Clinical applications of anterior segment optical coherence tomography. *J Ophthalmol* 2015; **2015**: 605729.
6 Ramos JL, Li Y, Huang D. Clinical and research applications of anterior segment optical coherence tomography - a review. *Clin Experiment Ophthalmol* 2009; **37**: 81–89.
7 Fujimoto JG, Huang D. Introduction to optical coherence tomography. In: Huang D, Duker JS *et al. Imaging the Eye from Front to Back with RTVue Fourier-Domain Optical Coherence Tomography*. SLACK Inc.: New Jersey, USA, 2010, pp 1–22.
8 Izatt JA, Hee MR, Swanson EA, Lin CP, Huang D, Schuman JS *et al*. Micrometer-scale resolution imaging of the anterior eye in vivo with optical coherence tomography. *Arch Ophthalmol* 1994; **112**: 1584–1589.
9 Wylegala E, Teper S, Nowinska AK, Milka M, Dobrowolski D. Anterior segment imaging: Fourier-domain optical coherence tomography versus time-domain optical coherence tomography. *J Cataract Refract Surg* 2009; **35**: 1410–1414.
10 Sharma N, Gupta S, Maharana P, Shanmugam P, Nagpal R, Vajpayee RB. Anterior segment optical coherence tomography-guided management algorithm for descemet membrane detachment after intraocular surgery. *Cornea* 2015; **34**: 1170–1174.
11 Rocha G. Use of the visante for anterior segment ocular coherence tomography. *Tech Ophthalmol* 2007; **5**: 67–77.
12 Dada T, Sihota R, Gadia R, Aggarwal A, Mandal S, Gupta V. Comparison of anterior segment optical coherence tomography and ultrasound biomicroscopy for assessment of the anterior segment. *J Cataract Refract Surg* 2007; **33**: 837–840.
13 Wang C, Xia X, Tian B, Zhou S. Comparison of fourier-domain and time-domain optical coherence tomography in the measurement of thinnest corneal thickness in keratoconus. *J Ophthalmol* 2015; **2015**: 402925.
14 Leitgeb R, Hitzenberger C, Fercher A. Performance of fourier domain vs. time domain optical coherence tomography. *Opt Express* 2003; **11**: 889–894.
15 Altaan SL, Gupta A, Sidney LE, Elalfy MS, Agarwal A, Dua HS. Endothelial cell loss following tissue harvesting by pneumodissection for endothelial keratoplasty: an ex vivo study. *Br J Ophthalmol* 2015; **99**: 710–713.
16 Dua HS, Faraj L, Said DG. Dua's layer: discovery, characteristics, clinical applications, controversy and potential relevance to glaucoma. *Expert Rev Ophthalmol* 2015; **10**: 531–547.
17 Shousha MA, Perez VL, Wang J, Ide T, Jiao S, Chen Q *et al.* Use of ultra-high-resolution optical coherence tomography to detect in vivo characteristics of Descemet's membrane in Fuchs' dystrophy. *Ophthalmology* 2010; **117**: 1220–1227.
18 Christopoulos V, Kagemann L, Wollstein G, Ishikawa H, Gabriele ML, Wojtkowski M *et al. In vivo* corneal high-speed, ultra high-resolution optical coherence tomography. *Arch Ophthalmol* 2007; **125**: 1027–1035.
19 Ferre LA, Nada O, Sherknies D, Boisjoly H, Brunette I. Optical coherence tomography anatomy of the corneal endothelial transplantation wound. *Cornea* 2010; **29**: 737–744.
20 Mencucci R, Favuzza E, Tartaro R, Busin M, Virgili G. Descemet stripping automated endothelial keratoplasty in Fuchs' corneal endothelial dystrophy: anterior segment optical coherence tomography and *in vivo* confocal microscopy analysis. *BMC Ophthalmol* 2015; **15**: 99.
21 Huang D, Li Y, Tang M. Interpretation of corneal images. In: Huang D, Duker SJ *et al. Imaging the Eye from Front to Back with RTVue Fourier-Domain Optical Coherence Tomography*. SLACK Inc.: New Jersey, USA, 2010, pp 39–46.
22 Siebelmann S, Hermann M, Dietlein T, Bachmann B, Steven P, Cursiefen C. Intraoperative optical coherence tomography in children with anterior segment anomalies. *Ophthalmology* 2015; **122**: 2582–2584.
23 Ide T, Wang J, Tao A, Leng T, Kymionis GD, O'Brien TP *et al.* Intraoperative use of three-dimensional spectral-domain optical coherence tomography. *Ophthalmic Surg Lasers Imaging* 2010; **41**: 250–254.